A Coupled Soil Moisture and Surface Temperature Prediction Model

F. ÁCS AND D. T. MIHAILOVIĆ

Department of Meteorology, Institute of Field and Vegetable Crops, Faculty of Agriculture, University of Novi Sad, Novi Sad, Yugoslavia

B. RAJKOVIĆ

Institute of Meteorology, Faculty of Natural Sciences, University of Belgrade, Beograd, Yugoslavia

(Manuscript received 9 April 1990, in final form 24 September 1990)

ABSTRACT

A model for soil moisture and soil surface temperature prediction for bare soil is considered in this paper. In describing evaporation rate, soil structure and moisture were taken into account as much as possible. Soil moisture prediction was carried out using Sellers' method. Hydraulic properties were determined using both known values for the given type of soil and the empirical equations of Clapp and Hornberger. Soil surface temperature prediction were made using the "force–restore" method. Sensible and latent heat fluxes were determined using a resistance representation taking into consideration atmospheric stablity.

The model results were compared with some field data of soil temperature and latent and sensible heat fluxes. The agreement between the model-calculated and the observed heat fluxes was fairly good. Soil moisture and temperature prediction were satisfactory, although an excessive drying occurred at the beginning of a five-day simulation period. Some sensitivity analyses were also made. The model formulation of latent heat flux was compared with the formulation of Philip. Tests were made for different values of "mean temperature" in the restore term.

Furthermore, the model is applicable for the calculation of sensible and latent heat fluxes provided that net radiation, air temperature, humidity, and wind velocity at screen height are available.

1. Introduction

Exchange processes of radiation, momentum, mass, and sensible and latent heats are determined by the state of boundary-layer atmosphere and surface properties. The parameters most frequently used for characterization of the state of the boundary-layer atmosphere are: wind velocity, air temperature, and humidity. Ground properties are described by: 1) parameters that are constant in time and variable in space, such as geographic position, soil and vegetation types, etc., and 2) parameters that are variable in time such as surface temperature and wetness and all other parameters that depend on those two.

Description of the properties of ground surface layer varies in complexity of dependence on model size (a GCM or a synoptic-scale model; a mesoscale or a 1D atmospheric boundary-layer model). Soil-state prediction can be done in multiple-layer models in which the heat conduction equation is solved using finite differences. These models usually have a large number of layers and can be computationally expensive. On the other hand, there are energy balance methods for a single insulated layer. As in Arakawa (1972), a prognostic equation for ground temperature depends entirely on the forcing. Some authors consider ground heat flux as proportional to net radiation heating (Nickerson and Smiley 1975). To use heat fluxes in the top ground layer in a more physical way, a "force–restore" concept has been introduced (Bhumralkar 1975; Blackadar 1976). Deardorff (1977) applied the method to the soil moisture flux to determine surface moisture concentration. He also extended this approach to model soil moisture in vegetation-covered ground when latent heat flux becomes dominant (Deardorff 1978), Soil is divided in to several layers, and conservation of mass is imposed for each layer. The choice of the number and depth of the layers should account for soil structure and the presence of plants, as in Sellers et al. (1986). Since hydraulic properties show power dependence on soil structure (Clapp and Hornberger 1978), the morphological structure of the ground also has to be accounted for as much as possible.

The objective of this study was to construct a soil moisture and temperature prediction model in which attention is paid to a better representation of evaporation flux as related to the morphological structure of the ground and its moisture. The model was con-

Corresponding author address: Dr. Ferenc Ács, Faculty of Agriculture, Institute of Field and Vegetable Crops, Department of Meteorology, University of Novi Sad, Veljak Vlahovica 2, 21000 Novi Sad, Yugoslavia.

structed for bare soil surface conditions. Subsequently, the model can be expanded into a vegetation model where the dependence between moisture exchange processes and soil structure is even more important because of an increased role of evapotranspiration.

2. Model description

Coupled heat and moisture representation should increase the accuracy of surface temperature prediction. Therefore, a description of the soil moisture submodel and its application follows.

a. Soil moisture model

The soil moisture prediction was made by Sellers' method (Sellers et al. 1986). The prognostic equations for the soil separated into three layers (Fig. 1) were

$$\frac{\partial W_1}{\partial t} = \frac{1}{\theta_{s1} D_1}\left(P - Q_{12} - \frac{1}{\rho_w} E\right), \quad (1)$$

$$\frac{\partial W_2}{\partial t} = \frac{1}{\theta_{s2} D_2}(Q_{12} - Q_{23}), \quad (2)$$

$$\frac{\partial W_3}{\partial t} = \frac{1}{\theta_{s3} D_3}(Q_{23} - Q_3), \quad (3)$$

where $W_i = \theta_i/\theta_{si}$ is soil moisture wetness of the ith soil layer, θ_i is its volumetric soil moisture ($m^3\ m^{-3}$) and θ_{si} is its volumetric soil moisture at saturation ($m^3\ m^{-3}$). It is assumed that the value of the last parameter is equal to the value of soil pore space; D_i is the thickness of the ith soil layer (m), ρ_w is the density of water ($kg\ m^{-3}$), P is the infiltration of precipitation ($m\ s^{-1}$), E is the rate of evaporation from the soil surface ($m\ s^{-1}$ or $kg\ m^{-2}\ s^{-1}$), $Q_{i,i+1}$ is the flow between the i and $i+1$ soil layers ($m\ s^{-1}$), and Q_i is the gravitational drainage from the bottom soil layer.

The water flow between adjoining soil layers is given by

$$Q_{i,i+1} = \bar{K}\left(2\frac{\psi_i - \psi_{i+1}}{D_i + D_{i+1}} + 1\right), \quad (4)$$

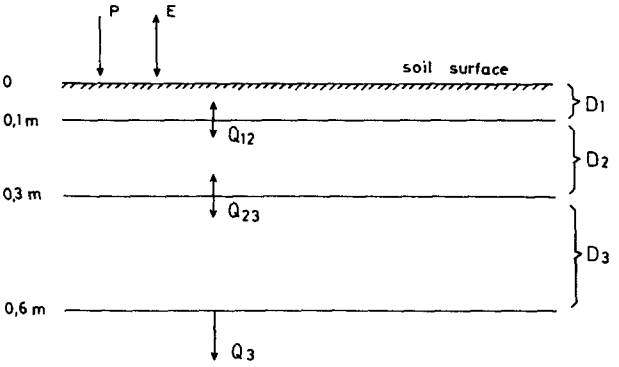

FIG. 1. Layers and water balance components used in the soil moisture prediction model.

TABLE 1. Structure description of the chernozem soil of the loess terrace of Southern Bačka to the depth of 60 cm.

Layer (cm)	Designation	Description
0–35	plow layer	Calcareous loam, dark brown, crumby–cloddy structure
35–60	subplow layer	Calcareous loam, dark brown, crumby–cloddy structure, occurrence of pseudomycelia at the depth of 50 cm

$$\bar{K} = \frac{D_i K_i + D_{i+1} K_{i+1}}{D_i + D_{i+1}}, \quad (5)$$

where $\bar{K}$ is an effective hydraulic conductivity between soil layers ($m\ s^{-1}$) and K_i is the hydraulic conductivity of the ith soil layer ($m\ s^{-1}$). The latter parameter was determined using Clapp–Hornberger's empirical formula (Clapp and Hornberger 1978)

$$K_i = K_{si} W_i^{2B_i+3}, \quad (6)$$

where K_{si} is the hydraulic conductivity at saturation of the ith soil layer ($m\ s^{-1}$). Furthermore, ψ_i is the soil moisture potential of the ith layer (m), also obtained by Clapp and Hornberger's empirical formula (Clapp and Hornberger 1978) as

$$\psi_i = \psi_{si} W_i^{-B_i}, \quad (7)$$

where ψ_{si} is the soil moisture potential at saturation (m) and B_i is an empirical constant of ith soil layer.

The gravitational drainage rate from the bottom is calculated by

$$Q_i = K_{si} W_i^{(2B_i+3)} \sin x, \quad (8)$$

where x is the mean slope angle, visually estimated to 3°.

Hydraulic and thermal properties of the soil are dependent on soil structure. In this study, simulation was made for the chernozem soil of the loess terrace of Southern Bačka. A description of its structure and its distribution were given by Vučić (Vučić 1964; Table 1 herein). Some of its hydraulic properties, namely soil pore space and hydraulic conductivity at saturation with pF curves, were also determined by Vučić (Vučić 1964). Using pF curves, which represent relationship between the logarithm of soil moisture potential and soil moisture wetness, and following Clapp and Hornberger's assumption that the relationship between the logarithm of soil moisture potential and the logarithm of soil moisture wetness is linear, we were able to determine the constants ψ_s and B for both layers as defined by Vučić. The hydraulic constants are presented in Table 2.

b. Soil surface temperature submodel

The soil surface temperature prediction was made using the force–restore method. This method takes into

TABLE 2. Hydraulic constants of the chernozem soil of the loess terrace of Southern Bačka.

Hydraulic properties of soil	Layer 0–30 cm	Layer 30–60 cm
Soil porosity ($m^3\ m^{-3}$)	0.5490	0.4880
Saturated hydraulic conductivity ($m\ s^{-1}$)	5.8×10^{-5}	0.89×10^{-5}
Saturated moisture potential (m)	−0.036	−0.085
Dimensionless constant B	6.50	7.26

consideration the soil heat flux exchange between the surface and deeper layers. We applied Bhumralkar's prognostic equation (Bhumralkar 1975; Fig. 2).

$$C_1 \frac{\partial T_g}{\partial t} = F(T_g) \tag{9}$$

where

$$C_1 = 2 \times 10^{-2} C + \left(\frac{\lambda C}{2\omega}\right)^{1/2}, \tag{10}$$

$$F(T_g) = S - R(T_g) - LE(T_g) - H(T_g) - \left(\frac{\omega C \lambda}{2}\right)^{1/2} (T_g - \bar{T}). \tag{11}$$

Here C_1 is the bulk heat capacity per unit area of the upper 2 cm of soil ($J\ m^{-2}\ K^{-1}$), C is the volumetric heat capacity ($J\ m^{-3}\ K^{-1}$), λ is the thermal conductivity ($W\ m^{-1}\ K^{-1}$), ω is the angular frequency (s^{-1}), $F(T_g)$ is the function of soil surface energy balance components ($W\ m^{-2}$), S is the shortwave radiation balance ($W\ m^{-2}$), $R(T_g)$ is the longwave radiation balance ($W\ m^{-2}$), L is the latent heat of water vaporization ($J\ kg^{-1}$), H is the sensible heat flux ($W\ m^{-2}$), T_g is the temperature in the upper 2 cm of soil (K), and $\bar{T}$ is the average daily temperature in the 2-cm surface soil layer (K).

c. Radiation balance

Net shortwave radiation is the difference between global and reflected radiation,

$$S = G_l - R_e. \tag{12}$$

Net longwave radiation was determined using the modified Angström's formula (Angström 1916)

$$R(T_g) = [\epsilon\sigma T_a^4 (0.180 + 0.250 \times 10^{-0.094 e_a}) + 4\epsilon\sigma T_a^3 (T_g - T_a)](1 - 0.70N), \tag{13}$$

where ϵ is the soil surface emissivity, σ is the Stefan–Boltzmann constant ($W\ m^{-2}\ K^{-4}$), T_a is the atmosphere temperature at screen height (K), e_a is the water vapor at screen height (mb), and N is the cloud cover in tenths. The constants used in Eq. (13) are the so-called Boltz–Falckenberg's constants (Boltz and Falckenberg 1949). They appeared to be appropriate for the calculation of net longwave radiation during both day and night.

d. Sensible and latent heat fluxes

Sensible and latent heat fluxes were determined using a "resistance" representation,

$$H = \rho C_p \frac{T_g - T_a}{r_a}, \tag{14}$$

$$LE = \frac{\rho C_p}{\gamma} \frac{f_h e_s(T_g) - e_a}{r_{surf} + r_a}, \tag{15}$$

respectively, where ρ is the air density ($kg\ m^{-3}$), C_p is the specific heat of air at constant pressure ($J\ kg^{-1}\ K^{-1}$), γ is the psychrometric constant ($mb\ K^{-1}$), and f_h is a dimensionless function that shows how far/close evaporation is from potential evaporation. We chose a linear dependence on $W_1 = \theta_1/\theta_{1max}$, i.e., the soil moisture wetness of the first layer. When it reaches 0.75 or more, the evaporation becomes potential and f_h is equal to 1, i.e.,

$$f_h = \begin{cases} W_1/0.75, & W_1 < 0.75 \\ 1, & W_1 > 0.75. \end{cases} \tag{16}$$

The value of 0.75 was chosen after Noilhan and Planton (1989), although their functional form of f_h (θ_1/θ_{1max}) was different. The linear form was chosen from Wetzel's (1978) plot, presenting a ratio for evaporation/potential evaporation versus W/W_{max}. The member $e_s(T_g)$ is saturation vapor pressure at temperature T_g calculated by the empirical formula

$$e_s(T_g) = 6.11 \exp\left[\frac{17.4(T - 273.16)}{T - 34.16}\right] \tag{17}$$

when T is in kelvin. Furthermore, r_{surf} is the surface resistance of bare soil ($s\ m^{-1}$) and r_a is the atmospheric resistance to water vapor and heat between roughness height and the reference level within the atmospheric layer with constant fluxes ($s\ m^{-1}$).

Atmospheric resistance depends on atmospheric stability. We determined it from temperature, wind speed, and turbulent transfer coefficients profiles in the atmospheric boundary layer. The procedure used is that due to Gourdiaan (Gourdiaan 1977). In neutral

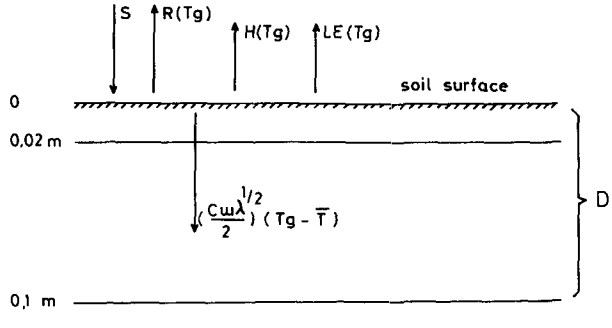

FIG. 2. Layers and energy balance components used in the soil surface temperature prediction model.

stratification the wind velocity profile varies logarithmically,

$$\bar{u}(z) = \frac{u_*}{k} \ln(z/z_0) \tag{18}$$

where $\bar{u}(z)$ is the average wind speed at height z (m s^{-1}), and z_0 is the roughness parameter (m). Given a value of 0.01 in the case of a bare soil surface, u_* is the friction velocity (m s^{-1}), and k is von Kármán's constant set at 0.40 in this study. The atmospheric resistance between levels z_0 and z_r (z_r is a reference level, as well as the level of atmospheric measurements in this study) is

$$r_a = \frac{0.74 \ln(z_r/z_0)}{ku_*}. \tag{19}$$

Combining the latter equation by the former, the atmospheric resistance may be easily calculated.

In nonneutral stratifications two parameters characterize the degree of nonneutrality, Richardson's number, and the Monin–Obukhov length. Both parameters relate buoyancy and shear forces. The gradient Richardson's number in the finite differences between the levels z_0 and z_r is

$$\mathrm{Ri}_g = -\frac{g(T_g - T_a)(z_r - z_0)}{T_{\mathrm{abs}} U_r^2}, \tag{20}$$

where T_{abs} is the absolute temperature assigned a constant value of 300 K, and u_r is the average wind speed at the level z_r. In Eq. (20) ground temperature was taken instead of the atmospheric temperature at the level z_0. The Monin–Obukhov length could be expressed as

$$L_{\mathrm{mon}} = \frac{T_{\mathrm{abs}} u_* \int_{z_0}^{z_r} \frac{\phi_n}{z}\, dz}{k^2 g(T_g - T_a)}, \tag{21}$$

where ϕ_h is a dimensionless temperature gradient function. It was expressed through the well-known Businger equation (Businger et al. 1971). The atmospheric resistance to heat transport between levels z_0 and z_r, as well as the friction velocity from the wind profile equation, were obtained through

$$r_a = \int_{z_0}^{z_r} \frac{\phi_h}{ku_* z}\, dz \tag{22}$$

and

$$u_* = \frac{ku_r}{\int_{z_0}^{z_r} \frac{\phi_m}{z}\, dz} \tag{23}$$

where ϕ_m is a dimensionless wind shear function. It was obtained using Businger's equations. The dimensionless height parameter ζ, ($\zeta = z/L_{\mathrm{mon}}$) between levels z_0 and z_r is

$$\Delta\zeta = \frac{z_r - z_0}{L_{\mathrm{mon}}}. \tag{24}$$

Parameter $\Delta\zeta$ for unstable stratification could be obtained only iteratively. A detailed description of the iterative procedure used is given in section 3a.

The determination of parameter $\Delta\zeta$ for stable stratification is simplier than for unstable stratification because Eqs. (23) and (21) could be solved analytically. Thus, we get

$$u_* = \frac{ku_r}{\ln(z_r/z_0) + 4.7\Delta\zeta} \tag{25}$$

and

$$L_{\mathrm{mon}} = -\frac{T_{\mathrm{abs}} u_* (0.74 \ln z_r/z_0 + 4.7\Delta\zeta)}{k^2 g(T_g - T_a)}. \tag{26}$$

Using Eqs. (24), (25), and (26), parameter $\Delta\zeta$ may be expressed as

$$\Delta\zeta = \frac{-b + (b^2 - 4ac)^{1/2}}{2a}, \tag{27}$$

where

$$a = 4.7(1 - 4.7\ \mathrm{Ri}_g) \tag{28}$$

$$b = (0.74 - 2 \times 4.7\ \mathrm{Ri}_g) \ln(z_r/z_0) \tag{29}$$

$$c = -\mathrm{Ri}_g \ln(z_r/z_0). \tag{30}$$

Thus, the parameter $\Delta\zeta$ could be obtained easily knowing Ri_g while L_{mon} is determined using Eq. (24). The friction velocity is calculated by Eq. (25) and the atmospheric resistance according to the equation

$$r_a = \frac{0.74 \ln(z_r/z_0) + 4.7\Delta\zeta}{ku_*}. \tag{31}$$

Neutral condition is assumed when Ri_g is between -0.001 and 0.001. For $\mathrm{Ri}_g > 1/4.7$, the value of the parameter $\Delta\zeta$ [Eq. (27)] becomes imaginary, which means that full inversion has occurred.

Surface resistance was calculated following Wetzel and Chang (1988) as

$$r_{\mathrm{surf}} = \frac{15}{u_*}. \tag{32}$$

e. Soil heat flux and thermal properties of the soil

In Eq. (11) the soil heat flux term is described by $(\omega c\lambda/2)^{1/2}(T_g - \bar{T})$. Instead of daily and layer-averaged temperature in the upper 2 cm of soil $\bar{T}$, the average daily soil temperature at the 2-cm depth was taken for $\bar{T}$. Volumetric heat capacity of the surface

layer depends on the volumetric soil moisture according to Lehtveer and Int (1977):

$$C = \rho_s(c + 4187\theta_1), \tag{33}$$

where ρ_s is the soil density (kg m^{-3}) and c is the specific heat of soil (J kg^{-1} K^{-1}). The value taken for soil density was 1.29×10^3 kg m^{-3} (Živković et al. 1972). The value chosen for the specific heat of the soil was 840 J kg^{-1} K^{-1}. Thermal conductivity was calculated using the expression

$$\lambda = K_T C, \tag{34}$$

where K_T is thermal diffusivity of soil (m^2 s^{-1}). In the surface layer, its value was 1.5×10^{-7} m^2 s^{-1} (Ács and Mihailović 1983).

3. Numerical experiment

a. Solution method

The mathematical–analytical procedure of determination of relevant parameters such as $\Delta\zeta$, u_*, and r_a for neutral and stable stratifications is given in section 2. For unstable stratifications, the procedure must be iterative. Its calculation algorithm follows.

1) The choice of initial value of $\Delta\zeta$ (in this study $\Delta\zeta = -0.21$);

2) The determination of Monin–Obukhov length using Eq. (24);

3) The calculation of dimensionless wind shear and temperature gradient functions $\phi_m(\zeta)$ and $\phi_h(\zeta)$, respectively, on the 20 equidistant levels between z_0 and z_r;

4) The calculation of integrals

$$I_m = \int_{z_0}^{z_r} \frac{\phi_m(z/L_{\text{mon}})}{z}\, dz$$

and

$$I_h = \int_{z_0}^{z_r} \frac{\phi_h(z/L_{\text{mon}})}{z}\, dz.$$

The integrals I_m and I_h are numericaly calculated using Simpson's formula;

5) The calculation of a new value of $\Delta\zeta$ using equation

$$\text{Ri}_g = \frac{\Delta\zeta I_h}{I_m^2}. \tag{35}$$

Equation (35), which connects the gradient Richardson number and dimensionless height parameter $\Delta\zeta$, is obtained by combining Eqs. (20), (21), (23), and (24); Ri_g is determined through Eq. (20). Iteration of the previous k steps continues until the difference of parameter $\Delta\zeta$ between two iterations is smaller than 0.0001;

6) The determination of Monin–Obukhov length, friction velocity, and atmospheric resistance. The final value of Monin–Obukhov length is obtained by using Eq. (24), while friction velocity and atmospheric resistance are determined by Eqs. (23) and (22), respectively.

The soil moisture prediction equations were solved using a forward time scheme. Distribution of the analyzed layers followed the soil structure distribution; thus, D_1 = 0–0.1 m, D_2 = 0.1–0.3 m, and D_3 = 0.3–0.6 m.

The soil surface temperature prediction equation is solved using an implicit scheme;

$$T_g^{t+\Delta t} = T_g^t + F_{(T_g)}^t \Big/ \left(\frac{c_1}{\Delta t} - \left.\frac{\partial F_{(T_g)}}{\partial T_g}\right|_t\right) \tag{36}$$

where function $\partial F_{(T_G)}/\partial T_g$ represents the change of soil surface energy balance components with soil surface temperature. The time step used was 900 s.

b. Experimental site and measurements

The experimental site was located on the meteorological station at Rimski Šančevi (45.33°N, 19.5°E), altitude of 84 m, on the chernozem soil of the loess terrace of Southern Bačka.

The prediction model was tested using two sets of data. The first set refers to 4 June 1982, chosen between the data that had been collected in the framework of gradient measurements performed for energy balance investigations above bare and wheat-planted soil surface in 1982. The second set refers to the period 15–20 April 1988, collected specifically for checking the accuracy of soil moisture and surface temperature predictions.

The initial conditions were obtained from measurements of soil temperatures at 2-cm depth and soil moisture content at 10-cm intervals up to 1-m depth. Soil temperatures were measured by mercury geothermometer and soil moisture content in wet and dry soil samples.

The boundary conditions were derived from hourly measurements of global and reflected radiation, cloudiness, precipitation, wet-bulb and dry-bulb temperatures at screen height, and average wind speed. Global and reflected radiation fluxes were registered by pyranometers installed 1.5 m above the soil surface. Measurements were recorded by a recording millivoltmeter with a drop-bar system manufactured by Kipp and Zonen. Other parameters were determined within the scope of standard meteorological observations. Soil temperatures at 2 cm were measured by mercury geothermometer at the local meteorological station at 0700, 1400, and 2100 LST and also by the authors at other hours to expand the experimental data.

c. Results and discussion

Accuracy of the calculated energy balance components was checked on a dataset collected in the frame-

work of gradient measurements. Soil heat fluxes calculated by the force–restore method have the usual daily course with extreme values up to 80 W m^{-2} (according to our convention, the negative sign denotes energy loss from the soil surface). Sensible and latent heat fluxes are compared to sensible and latent heat fluxes calculated by the Bowen ratio method (Figs. 3 and 4). In the Bowen ratio method, latent heat flux was calculated by the formula $LE = [S - R(T_g) - G]/(1 + \beta)$, where G is soil heat flux, estimated from gradient measurement of soil temperatures using Cejtin's method (Cejtin 1953), and β is the Bowen ratio H/LE. The member β was obtained from gradient measurements of air temperature and vapor pressure within the surface boundary layer. The gradient measurements were performed using platinum resistance thermometers (measurements accuracy 0.1°C). The thermometers were set at 0.2, 0.5, 0.8, 1.1, 1.4, 1.7, and 2 m above soil surface to minimize the experimental error. Namely, it is desirable to measure air temperature and vapor pressure at six or more heights above the surface, so that good average values of β can be derived from the profile (Monteith 1973). In spite of this, the signs of gradients observed and the fluxes calculated were opposite in some cases, mainly near sunset, presumably because of the momentary measurements. In these cases, the fluxes obtained by the Bowen ratio method were not presented. Largest variations of sensible heat fluxes were observed early in the morning and at 1300 LST ranging from 60 to 80 W m^{-2}. The variations of latent heat fluxes were somewhat larger than the variations of sensible heat fluxes. The maximum variation was 130 W m^{-2} and was observed at 1000 LST.

The prediction was made for the period 15–20 April 1988. It started at 1200 LST 15 April and ended at 1200 LST 20 April. Before the experimental period, the soil suface layer was wet. On 13 April there was 6 mm rain. In this period, the weather was very changeable. At the beginning, "košava," a strong local wind

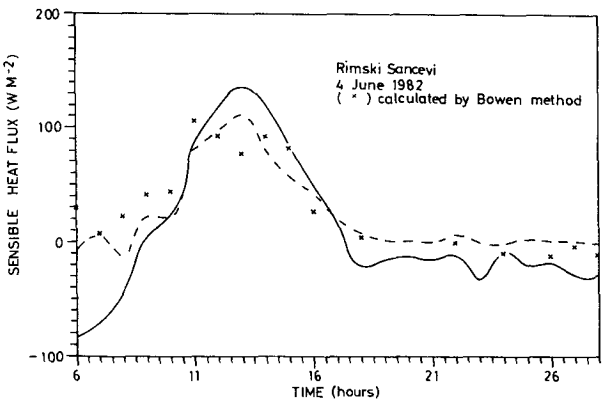

FIG. 3. Diurnal changes of sensible heat fluxes calculating the dimensionless function f_h by the authors' (solid line) and Philip's (dashed line) formulas.

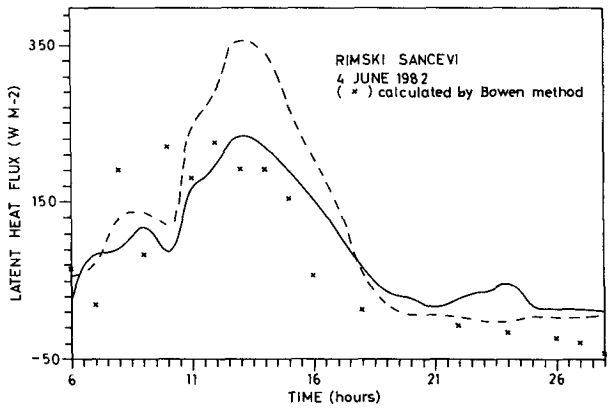

FIG. 4. As in Fig. 3, but for latent heat fluxes.

from the southeast, was blowing with speeds up to 11 m s^{-1}. The average daily air temperatures were low, about 3.5°C. A few days later the košava abated, and the daily average air temperatures rose somewhat to about 10°–13°C. Up to the end of the period, a gradual temperature rise was observed.

The five-day course of soil moisture content prediction is presented in Fig. 5. The figure shows considerable drying, especially in the surface soil layer (0–10 cm); the predicted value is lower than the observed one by 0.025 m^3 m^{-3}.

The daily periodic character of soil moisture changes in this layer was noticeable. Daily cycles of drying and humidifying were also evident. On days without precipitation (18 and 19 April), drying processes were pronounced and the soil moisture content decrease was about 0.015 m^{-3} m^{-3}. The only exception was 15 April, when the soil moisture reduction was about 0.020 m^{-3} m^{-3}. This initial drying contributed most to the total drying. In the days with precipitation (0.4 mm between 1700 and 1900 LST 16 April, indicated with arrows on Fig. 5, and 0.1 mm between 0600 and 0700 LST 17 April, also indicated with arrows), the drying effect was about one-half times lower. The daily cycles of drying and humidifying had nearly the same durations. The drying period lasted from 0800 to 2000 LST and

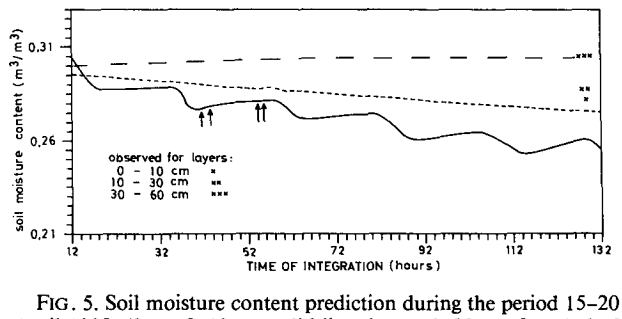

FIG. 5. Soil moisture content prediction during the period 15–20 April 1988, (layer 0–10 cm solid line; layer 10–30 cm fine dashed line; layer 30–60 cm coarse dashed line). Arrows show periods with precipitation.

the humidifying period from 2000 to 0800 LST of the next day. In the 10–30 cm layer, soil moisture content decreased linearly.

The five-day 2-cm soil surface temperature prediction is presented in Fig. 6. The prediction was made using constant $\bar{T}$ from 14 April 1988. The differences between predicted and observed values were highest about noon, 3–5 K. Differences were smaller in the morning and afternoon when their values were up to 2–3 K.

Sensitivity of the soil moisture prediction is determined to a great extent by the dimensionless function f_h. Replacing (16) by Philip's formula (Philip 1957) for the dimensionless function f_h, separate tests were made to check the sensible and latent heat fluxes and soil moisture prediction. According to Philip's formula:

$$f_h = \begin{cases} \exp(\psi_1 g / R_v T_g), & e_s(T_g) > e_a \\ 1, & e_s(T_g) < e_a, \end{cases} \quad (40)$$

where ψ_1 is soil surface moisture potential (m), g is acceleration of gravity (m s^{-2}), and R_v is the gas constant for water vapor (J kg^{-1} K^{-1}).

The obtained sensible and heat fluxes compared with those calculated by Eq. (16) and by the Bowen method, are presented in Figs. 3 and 4, respectively. Variations between sensible heat fluxes calculated by the two formulas were highest early in the morning, but they did not exceed 80 W m^{-2}. The agreement between sensible heat fluxes calculated by Philip's formula and by the Bowen method was better than in the case of application of Eq. (16), mainly in the early morning. Variations between latent heat fluxes were much higher than the variations between sensible heat fluxes, regardless of which formula was used. The maximum variation amounted to 120 W m^{-2} at 1300 LST. Latent heat fluxes during the day, calculated by our formula, were in better agreement with the values calculated by the Bowen method than by the Philip's formula. The situation was reversed for the calculation of latent heat fluxes at night.

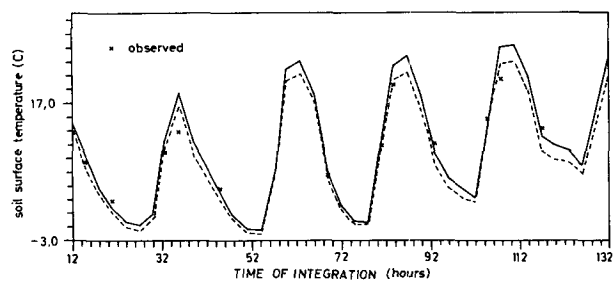

FIG. 6. Temperature prediction for the 2-cm soil surface layer performed calculating the dimensionless function f_h by the authors' (solid line) and Philip's (dashed line) formulas during the period 15–20 April 1988.

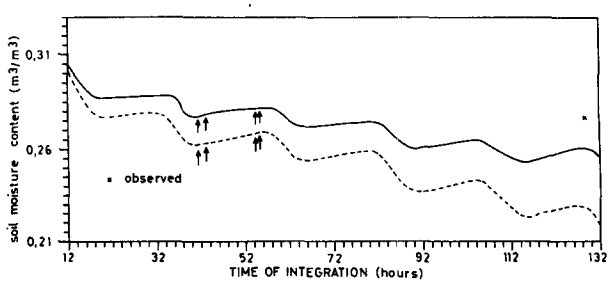

FIG. 7. Soil moisture prediction in soil surface layer (0–10 cm) calculating the dimensionless function f_h by the authors' (solid line) and Philips' (dashed line) formulas during the period 15–20 April 1988. Arrows show periods with precipitation.

The most significant changes in soil moisture prediction were induced in the soil surface layer (0–10 cm). The soil moisture predictions were performed separately using the formulas of the authors and Philip for the soil surface layer, and are presented in Fig. 7. The drying effect was more conspicuous for the Philip's formula than for Eq. (16). This is easily explained by the variations between latent heat fluxes calculated by Philip's and our formula, especially near noon. Naturally, changes in five-day temperature prediction for the 0–2 cm soil layer could also be observed (Fig. 6). The deviations between predicted temperatures for Philip's and our formulas ranged from 0° to 3°C; the temperatures predicted by Eq. (16) were unanimously higher than those predicted by the Philip's formula.

The sensitivity of the soil surface temperature prediction model is investigated on the basis of changes of average daily soil temperature at a 2-cm depth $\bar{T}$. Diurnal changes of sensible and latent heat fluxes for different values of parameter $\bar{T}$ are presented in Figs. 8 and 9, respectively. Changes of parameter $\bar{T}$ of 5°C caused maximum changes of sensible and latent heat fluxes up to 40–70 W m^{-2}.

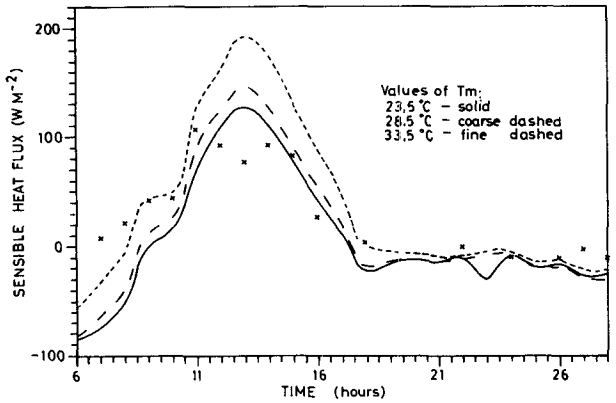

FIG. 8. Diurnal change of sensible heat fluxes for different values of average daily soil temperature at 2-cm depth, $\bar{T}$.

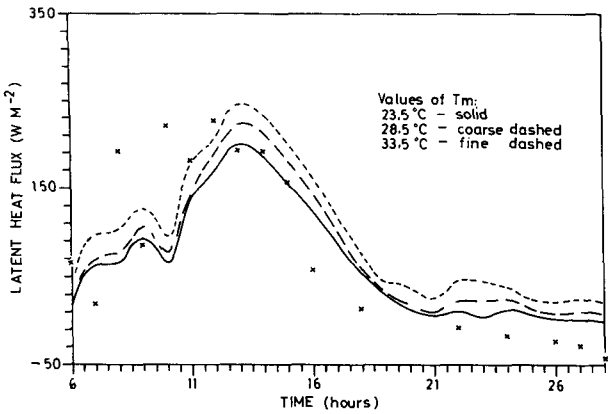

FIG. 9. As in Fig. 8, but for latent heat fluxes.

The soil surface temperature prediction model was fairly insensitive to any change of parameter $\bar{T}$. This is shown in Fig. 10 where the 2-cm soil surface temperature predictions for the period 15–20 April are presented for:

(i) $\bar{T}$ on 14 April 1988,
(ii) changeable $\bar{T}$ during the period where $\bar{T}$ refers to the day before the day the prediction is made, and
(iii) changeable $\bar{T}$ during the period where $\bar{T}$ refers to the day the prediction is made.

The differences between the soil surface temperatures predicted for different $\bar{T}$ are small, 1°–2°C on average. They are largest at daybreak 19 April when the temperature differences reached 4°C. These facts prove that soil surface temperature prediction could be done reliably by a constant $\bar{T}$ parameter that refers to the day before the prediction period.

Sensitivity of the soil moisture prediction model to the change of average daily soil temperature at a 2 cm

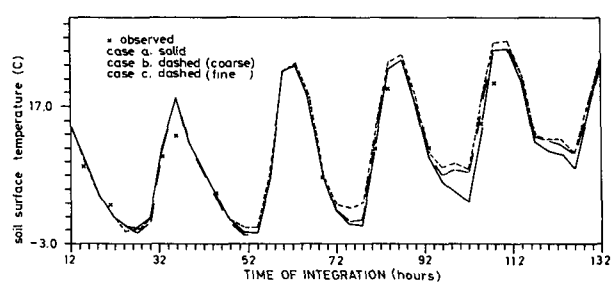

FIG. 10. Temperature prediction for 2-cm soil surface layer during the period 15–20 April 1988 for (a) T of 14 April 1988, (b) changeable $\bar{T}$ during the period where $\bar{T}$ refers to the day previous to the day for which the prediction is made, and (c) changeable $\bar{T}$ during the period where $\bar{T}$ refers to the day for which the prediction is made.

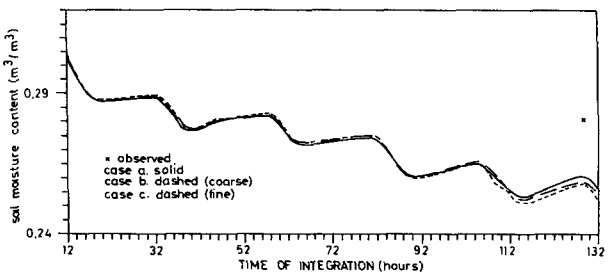

FIG. 11. As in Fig. 10, but for soil moisture prediction.

depth was not high, as shown in Fig. 11, where soil moisture predictions for the same changes of parameter $\bar{T}$ as in the case of soil surface temperature prediction are presented. Naturally, the greatest differences were between cases (i) and (iii) when the difference at the end of the period is 0.0040 m^3 m^{-3}.

4. Conclusion

A bare soil moisture and soil surface temperature prediction model is presented. The model was tested separately by the data observed on 4 June 1982 and during the period 15–20 April 1988 for a specific soil type. Accuracy of the calculated sensible and latent heat fluxes was tested using the 1982 data. It was shown that agreement between the calculated and observed heat fluxes was fairly good. Thus, the model could be used for the calculation of sensible and latent heat fluxes. Soil moisture predictions are satisfactory in spite of excessive drying at the beginning of the five-day simulation period. Soil surface temperature predictions are also satisfactory; the maximum differences between the predicted and the observed values never exceeded 5°C. Nevertheless, due to limited experimental data on soil moisture wetness, no definite conclusion about the quality of the proposed parameterization can be made.

The sensitivity analysis showed that both soil moisture and soil surface temperature prediction models are sensitive to the formulation of latent heat flux and insensitive to changes of average daily temperature of surface soil layer. Replacing the authors' formula by Philip's formula for the dimensionless function f_h, soil moisture prediction deteriorated, especially in the surface layer, but the 2-cm soil layer temperature prediction was improved. Soil surface temperature predictions were insensitive to the changes of average daily temperature of the surface soil layer $\bar{T}$. Therefore, soil surface temperature prediction could be done reliably by constant $\bar{T}$ parameter, which referred to the day before the prediction period, independent of the length of this period.

APPENDIX

List of Symbols

1. Constants

Name	Symbol	Value	Units
Time step	Δt	900	s
Thickness of ith soil layer	D_i		m
Angular frequency	ω	72.7×10^{-6}	s^{-1}
Stefan–Boltzmann constant	σ	5.57×10^{-3}	W m^{-2} K^{-4}
Acceleration of gravity	g	9.81	m s^{-2}
Roughness parameter	z_0	0.01	m
Reference level	z_r	2	m
Initial value of dimensionless height parameter in finite difference	$\Delta\zeta$	−0.21	
Psychrometric constant	γ	0.65	mb K^{-1}
Absolute temperature	T_{abs}	300	K
Gas constant for water vapor	R_v	461	J kg^{-1} K^{-1}
Latent heat of vaporization of water	L	2.5×10^6	J kg^{-1}
von Kármán constant pressure	k	0.04	
Specific heat of air at constant	c_p	1004	J kg^{-1} K^{-1}
Air density	ρ	1.20	kg m^{-3}
Density of water	ρ_w	1000	kg m^{-3}
Soil surface emissivity	ϵ	0.96	
Specific heat of soil	c	840	J kg^{-1} K^{-1}
Density of soil	ρ_s	1.29×10^3	kg m^{-3}
Average daily soil temperature at 2-cm depth	$\bar{T}$		K
Thermal diffusivity of soil surface layer	K_T	1.5×10^{-7}	m^2 s^{-1}
Mean slope angle	x	3	deg
Volumetric soil moisture at saturation	θ_{si}	Layer 0–30 cm 0.5490 Layer 30–60 cm 0.4880	m^3 m^{-3}
Hydraulic conductivity at saturation	K_{Si}	Layer 0–30 cm $0.89\ 10^{-5}$ Layer 30–60 cm $0.93\ 10^{-5}$	m s^{-1}
Soil moisture potential at saturation	ψ_{si}	Layer 0–30 cm −0.036 Layer 30–60 cm −0.085	m
Empirical constant	B_i	Layer 0–30 cm 6.50 Layer 30–60 cm 7.26	

2. Quantity

Name	Symbol	Units
Height or depth	z	m
Time	t	s
Shortwave radiation balance	S	W m^{-2}
Global radiation	G_l	W m^{-2}
Reflected radiation	R_e	W m^{-2}
Longwave radiation balance	$R(T_g)$	W m^{-2}
Function of soil surface energy balance	$F(T_g)$	W m^{-2}

2. Quantity

Name	Symbol	Units
Atmosphere temperature at screen height	T_a	K
Water vapor at screen height	e_a	mb
Cloudiness	N	
Rate of evaporation	E	kg m^{-2} s^{-1} or m s^{-1}
Sensible heat flux	H	W m^{-2}
Bowen ratio		
Saturation vapor pressure at temperature T_g	$e_s(T_g)$	mb
Surface resistance of bare soil	r_{surf}	s m^{-1}
Atmospheric resistance	r_a	s m^{-1}
Average wind speed at height z	$u(z)$	m s^{-1}
Friction velocity	u_*	m s^{-1}
Average wind speed at level z_r	u_r	m s^{-1}
Gradient Richardson's number	Ri_g	
Monin–Obukhov length	L_{mon}	m
Dimensionless height parameter	ζ	
Dimensionless temperature gradient function	ϕ_h	
Dimensionless wind shear function	ϕ_m	
Dimensionless height parameter in finite difference	$\Delta\zeta$	
Temperature of 2-cm soil surface layer	T_g	K
Volumetric heat capacity of soil	C	J m^{-3} K^{-1}
Heat capacity per unit area of 0–2 cm soil surface layer	C_1	J m^{-2} K^{-1}
Thermal conductivity		W m^{-1} K^{-1}
Soil moisture wetness of ith soil layer	W_i	
Volumetric soil moisture of ith soil layer		m^3 m^{-3}
Infiltration rate of precipitation	P	m s^{-1}
Soil water flow between i and $i+1$ soil layer	$Q_{i,i+1}$	m s^{-1}
Gravitational drainage from the bottom soil lay	Q_i	m s^{-1}
Hydraulic conductivity of ith soil layer	K_i	m s^{-1}
Effective hydraulic conductivity between soil layers	$\bar{K}$	m s^{-1}
Soil moisture potential of ith soil layer	ψ_i	m
Dimensionless function	f_h	

REFERENCES

Ács, F., and D. T. Mihailović, 1983: Calculation of soil thermal changes. *Időjárás*, **4**, 200–205.

Angström, A., 1916: Über die Gegenstrahlung der Atmosphäre. *Meteorol. Z.*, **33**.

Arakawa, A., 1972: Design of the UCLA General Circulation Model. Simulation of weather and climate, Tech. Rep. No. 7, Department of Meteorology, University of California at Los Angeles, 116 pp.

Bhumralker, C. M., 1975: Numerical experiments on the computation of ground surface temperature in an atmospheric general circulation model. *J. Appl. Meteor.*, **14**, 1246–1258.

Blackadar, A. K., 1976: Modeling the nocturnal boundary layer. *Proceedings of the Third Symposium on Atmospheric Turbulence, Diffusion, and Air Quality*, Raleigh, Amer. Meteor. Soc., 46–49.

Boltz, R., and G. Falckenberg, 1949: Neubestimmung der Konstanten der Angströmschen Strahlunsformel. *Z. Meteorol.* **97.**

Businger, J. A., J. C., Wyngaard, Y. I. Izumi and E. F. Bradley, 1971: Flux-profile relationships in the atmospheric surface layer. *J. Atmos. Sci.*, **28**, 181–189.

Cejtin, G. H., 1953: K voprosu ob opredelenii nekotornjih teplovjih svojstv počvi. *Tr. GGO. Vljipusk*, **39**, 201.

Clapp, R. B., and G. M. Hornberger, 1978: Empirical equations for

some soil hydraulic properties. *Water Resour. Res.*, **14,** 601–604.

Deardorff, J. W., 1977: A parameterization of ground surface moisture content for use in atmospheric prediction models. *J. Appl. Meteor.*, **16,** 1182–1185.

——, 1978: Efficient prediction of ground surface temperature and moisture with inclusion of a layer of vegetation. *J. Geophy. Res.*, **83,** 1889–1903.

Goudriaan, J., 1977: *Crop Micrometeorology: A Simulation Study.* Wageningen Center for Agricultural Publishing and Documentation, 103 pp.

Lehtveer, R. V., and L. E. Int, 1977: Ob izmenchivosti osnovnih faktorov opredelayshih teplovoy rezim pochvi. *Trudy GG,* VYP. Gidrometeoizdat, **385,** 87–93.

Monteith, J. L., 1973: *Principles Environmental Physics.* Edward Arnold, 118 pp.

Nickerson, E. C., and E. V. Smiley, 1975: Surface energy budget parameterizations for urban scale models. *J. Appl. Meteor.*, **14,** 297–300.

Noilhan J., and S. Planton, 1989: A simple parameterization of land surface processes for meteorological models. *Mon. Wea. Rev.*, **117,** 536–500.

Philip, J. R., 1957: Evaporation and moisture and heat fields in the soil. *J. Meteor.*, **14,** 354–366.

Sellers, P. J., Y. Mintz, Y. C. Sud and A. Dalcher, 1986: A simple biosphere model (SIB) for use within general circulation models. *J. Atmos. Sci.*, **43**(7), 505–531.

Vučić, N., 1964: Water properties of chernozem and chernozem-like meadow soil and their significance for irrigation on the irrigated area of Bačka. *Contemporary Agriculture,* (special issues) **1**.

Wetzel, P. J., 1978: A detailed parameterization of the atmospheric boundary layer. Ph.D. dissertation, Colorado State University, (Also available as Atmospheric Science Paper No. 302.)

——, and Yui-Tai Chang, 1988: Evapotranspiration from nonuniform surfaces: A first approach for short-term numerical weather prediction. *Mon. Wea. Rev.* **116**(3), 600–621.

Živković B., and I. Sar., 1972: Zemljišta Vojvodine. Institute za PoljoPrivredna Istraživanja, Novi Sad, 684 pp.